

Waveform Design for Kalman Filter-Based Target Scattering Coefficient Estimation in Adaptive Radar System

Peng Chen ¹, Member, IEEE, Chenhao Qi ¹, Senior Member, IEEE, Lenan Wu, and Xianbin Wang ², Fellow, IEEE

Abstract—The temporal correlation of target can be exploited to improve the radar estimation performance. This paper studies the estimation of target scattering coefficients in an adaptive radar system, and a novel estimation method based on Kalman filter (KF) with waveform optimization is proposed for the temporally correlated target in the scenario with both noise and clutter. Different from the existing indirect methods, a direct optimization method is proposed to design the transmitted waveform and minimize the mean square error of the KF estimation. Additionally, the waveform is optimized subject to the practical constraints including the transmitted energy, the peak-to-average power ratio, and the target detection performance. With clutter and noise, the waveform optimization problem is non-convex. Therefore, a novel two-step method is proposed and converts the original non-convex problem into several semidefinite programming problems, which are convex and can solve efficiently. Simulation results demonstrate that the proposed KF-based method with waveform optimization can outperform state-of-art methods and significantly improve the estimation performance.

Index Terms—Adaptive radar system, Kalman filter, non-convex optimization, waveform optimization.

I. INTRODUCTION

IN ADAPTIVE radar systems, the transmitted waveforms can be optimized according to the radar working environment, so the better detection and estimation performance can be achieved than that with fixed waveforms [1]–[3]. Usually,

Manuscript received October 9, 2017; revised March 11, 2018 and July 4, 2018; accepted October 2, 2018. Date of publication October 10, 2018; date of current version December 14, 2018. This work was supported in part by the National Natural Science Foundation of China under Grants 61801112, 61871119, 61471117, and 61601281, in part by the Natural Science Foundation of Jiangsu Province under Grants BK20180357 and BK20161428, in part by the Open Program of State Key Laboratory of Millimeter Waves at Southeast University under Grant Z201804, and in part by the Fundamental Research Funds for the Central Universities. The review of this paper was coordinated by Dr. O. Holland. (Corresponding author: Chenhao Qi.)

P. Chen is with the State Key Laboratory of Millimeter Waves, Southeast University, Nanjing 210096, China and also with the Department of Electrical Engineering, Columbia University, New York, NY 10027 USA (e-mail: chenpengseu@seu.edu.cn).

C. Qi and L. Wu are with the School of Information Science and Engineering, Southeast University, Nanjing 210096, China (e-mail: qch@seu.edu.cn; wuln@seu.edu.cn).

X. Wang is with the Department of Electrical and Computer Engineering, Western University, London, ON N6A 3K7, Canada (e-mail: xianbin.wang@uwo.ca).

Color versions of one or more of the figures in this paper are available online at <http://ieeexplore.ieee.org>.

Digital Object Identifier 10.1109/TVT.2018.2875314

when the target is large enough to occupy more than one resolution cells, the echo signals from the different resolution cells are superimposed. Therefore, it is more appropriate to describe this type of target as an extended target [4] instead of a point target [5]–[7]. Under the assumption of a linear time-invariant target, target impulse response (TIR) is adopted to characterize the extended target [8], [9]. In [10], [11], this assumption is further extended to a wide sense stationary uncorrelated scattering (WSSUS) model, where the TIRs from different resolution cells are uncorrelated and temporally stationary.

In the adaptive radar systems, the transmitted waveforms can be optimized with the information of target and clutter to improve the radar performance, and most kinds of literature focus on the following two scenarios [12]:

- 1) The statistical information about the target scattering coefficients (TSC) or the clutter scattering coefficients (CSC) is assumed to be known, such as the power spectral density (PSD), the subspaces and the covariance matrices. For example, the waveform is optimized to maximize the worst-case signal-to-interference-and-noise ratio (SINR) in the colocated multiple-input and multiple-output (MIMO) radar [13], where the cyclic optimization algorithm based on the rank-one relaxation and the semidefinite programming (SDP) [14] is proposed. The waveform optimization method based on the TSC subspace is investigated in [15], [16]. Additionally, to jointly optimize the transmitted waveform and the receiving filter in the MIMO radar, an iterative method is proposed to maximize the detection performance for extended target in [17]. In the scenario with moving target, the joint optimization method based on cyclic maximization is also proposed to maximize the detection performance [18]. With the orthogonal waveforms, a weighting matrix is obtained to maximize SINR in [19].
- 2) The exact TSC or CSC are assumed to be known during the waveform optimization processes. For example, the transmitted waveforms are optimized in [20] to maximize the target detection performance, using a cosine function to generate the Toeplitz matrix. The waveform optimization method is also proposed in [21] for the multiple extended targets with the compressed sensing-based estimation method. The antenna placements are optimized

in [22] to improve the target localization performance with the target information.

For the temporally correlated targets, the Kalman filter (KF)-based method can be adopted to improve the TSC estimation performance, but the corresponding method of waveform optimization has not been proposed to improve the estimation performance, especially in the practical scenarios with the clutter and the waveform constraints [23].

The current optimization methods focus on maximizing the general parameters such as SINR or the mutual information to improve the TSC estimation performance [24], [25], but few methods are studied for the specific estimation methods. Additionally, for the practical scenarios, the following constraints must also be considered in waveform optimization:

- 1) *The constant envelope of the transmitted waveform:* it improves the power efficiency and takes full advantage of the nonlinear power amplifiers, especially in the multi-carrier radar systems [26]–[28]. Additionally, a peak-to-average power ratio (PAPR) is adopted as a relaxed form of the constant envelope constraint [29].
- 2) *The detection performance:* it is based on the constant false alarm rate (CFAR) detector [30], [31].
- 3) *The energy of transmitted waveform:* it is an essential constraint in the waveform optimization.

However, the waveform optimization for the temporally correlated target subject to these constraints has not been studied in the existing kinds of literature. Therefore, this paper focuses on improving the KF estimation performance by optimizing the transmitted waveform directly under these practical constraints.

In this paper, a novel KF-based method with optimized waveform is studied to estimate the TSC in an adaptive radar system with clutter. Different from existing indirect methods, a direct waveform optimization method is proposed. To minimize the mean square error (MSE) of the KF estimation at each iteration, we formulate a waveform optimization problem subject to the constraints of the transmitted energy, the PAPR, and the detection performance. Since the original problem of waveform optimization is non-convex and cannot be solved efficiently, a novel two-step method is proposed to convert it into several convex problems, which can be solved efficiently by the toolboxes. For the first step, an initial optimization waveform is obtained in the scenario without clutter by converting the original non-convex optimization problem into an SDP problem. For the second step with clutter, an iterative method is proposed to update this waveform. Finally, the optimized waveform in the scenario with both noise and clutter is obtained. To summarize, we make the contributions as follows:

- *Radar application:* The adaptive radar system is realized by optimizing the transmitted waveforms with the information of target and clutter, and the estimation method is combined with the corresponding waveform optimization processes. Different from the general optimization methods to maximize the SINR or mutual information of the received signals, the proposed method is a specific and direct optimization method for the KF-based estimator.

- *The direct waveform optimization method:* Different from the existing indirect methods, a direct method is proposed to optimize the transmitted waveforms for the KF-based estimator.
- *The practical waveform constraints:* For the practical consideration, the constraints including the transmitted energy, the PAPR and the detection performance are considered during the processes of waveform optimization.
- *The method to solve non-convex optimization problem:* With additional constraints, the original waveform optimization method is non-convex, and cannot be solved efficiently, so a two-step method is proposed to convert the non-convex problem into several convex ones.

The remainder of this work is organized as follows. In Section II, the radar system model is given and the method based on KF is proposed to estimate TSC in the scenario with clutter. Section III formulates the waveform design as a non-convex optimization problem, and a two-step method is proposed in Section IV. Simulation results are given in Section V. Finally, Section VI concludes the paper.

Notations: Symbols for matrices (upper case) and vectors (lower case) are in boldface. $(\cdot)^H$, $\text{diag}\{\cdot\}$, \mathbf{I}_L , $\mathcal{CN}(0, \mathbf{R})$, $|\cdot|$, $\|\cdot\|_2$, $\mathcal{E}\{\cdot\}$, $\text{Tr}\{\cdot\}$ and \mathcal{R} denote the conjugate transpose (Hermitian), the diagonal matrix, the identity matrix of size L , the complex Gaussian distribution with zero mean and covariance being \mathbf{R} , the absolute value, the ℓ_2 norm, the expectation, the trace of a matrix and the real part, respectively.

II. SYSTEM MODEL

As shown in Fig. 1, the target is described by an extended model, which can be expressed by either TIR in the time domain or TSC in the frequency domain. The echo signal from the target is interfered by that from clutter, which can be described by either clutter impulse response (CIR) in the time domain or CSC in the frequency domain. To ensure the consistency of results in the time domain and frequency domain, the length of a signal in time domain is M' and we extend it to M via adding zeros, where $M \geq 2M' - 1$. During the k -th pulse, the transmitted waveform is denoted as a vector $\mathbf{s}_k \in \mathbb{C}^{M \times 1}$, where M is the length of the discretized signal. Thus, in the scenario with clutter, the received signal $\mathbf{y}_k \in \mathbb{C}^{M \times 1}$ can be obtained in the frequency domain as

$$\mathbf{y}_k = \mathbf{Z}_k (\mathbf{g}_{T,k} + \mathbf{g}_C) + \mathbf{w}, \quad k = 1, 2, \dots \quad (1)$$

where the transmitted signals are described by a diagonal matrix in the frequency domain $\mathbf{Z}_k \triangleq \text{diag}\{\mathbf{z}_k\}$ and the diagonal entries of \mathbf{Z}_k are from a vector $\mathbf{z}_k \triangleq \mathbf{F} \mathbf{s}_k$. The Fourier matrix \mathbf{F} is defined as

$$\mathbf{F} \triangleq \frac{1}{\sqrt{M}} \begin{bmatrix} 1 & 1 & \dots & 1 \\ 1 & e^{-j2\pi \frac{1}{M}} & \dots & e^{-j2\pi \frac{M-1}{M}} \\ 1 & e^{-j2\pi \frac{2}{M}} & \dots & e^{-j2\pi \frac{2(M-1)}{M}} \\ \vdots & \vdots & \ddots & \vdots \\ 1 & e^{-j2\pi \frac{M-1}{M}} & \dots & e^{-j2\pi \frac{(M-1)(M-1)}{M}} \end{bmatrix}. \quad (2)$$

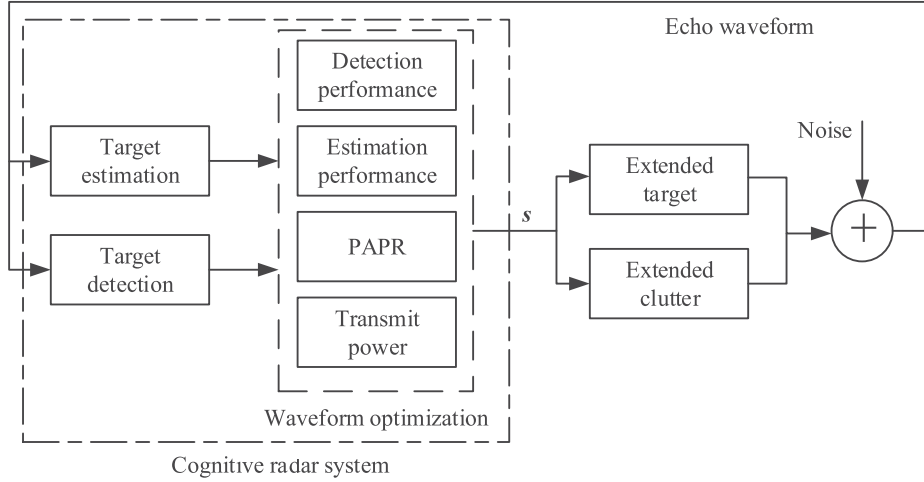


Fig. 1. The radar system with extended target and clutter.

\mathbf{w} denotes the additive Gaussian noise. $\mathbf{g}_{T,k} \triangleq \mathbf{F}\mathbf{h}_{T,k}$ and $\mathbf{g}_C \triangleq \mathbf{F}\mathbf{h}_C$ denote the TSC and CSC, respectively; $\mathbf{h}_{T,k} \in \mathbb{C}^{M \times 1}$ and $\mathbf{h}_C \in \mathbb{C}^{M \times 1}$ denote the TIR and CIR, respectively. Suppose $\mathbf{g}_{T,k} \sim \mathcal{CN}(\mathbf{0}, \mathbf{R}_T)$, $\mathbf{g}_C \sim \mathcal{CN}(\mathbf{0}, \mathbf{R}_C)$ and $\mathbf{w} \sim \mathcal{CN}(\mathbf{0}, \mathbf{R}_N)$, where \mathbf{R}_T , \mathbf{R}_C and \mathbf{R}_N denote the covariance matrix of the target, clutter and noise, respectively. The assumption of $\mathbf{g}_C \sim \mathcal{CN}(\mathbf{0}, \mathbf{R}_C)$ is common in radar systems, where \mathbf{R}_C can be estimated by the well-developed methods [32], [33].

Considering the extended target with slowly varying TIR, the TIR has a high correlation with the most recent TIR and less correlation with the older TIR. Therefore, a classically exponential correlated model has been proposed to describe the dynamic character of TIR in time domain [10], [11], [34]

$$\mathbf{h}_{T,k} = e^{-T_r/\tau} \mathbf{h}_{T,k-1} + \mathbf{u}_{k-1}, \quad (3)$$

where T_r denotes the pulse repetition interval (PRI), τ denotes the temporal decay constant describing the temporal TIR correlation between two neighboring pulses, and $\mathbf{u}_{k-1} \sim \mathcal{CN}(\mathbf{0}, (1 - e^{-2T_r/\tau})\mathbf{R}'_T)$ denotes a zero-mean Gaussian vector with covariance matrix $(1 - e^{-2T_r/\tau})\mathbf{R}'_T$, with $\mathbf{R}'_T \triangleq \mathbf{F}^H \mathbf{R}_T \mathbf{F}$ being the covariance matrix of $\mathbf{h}_{T,k}$. τ can be estimated by the estimation methods including maximum likelihood (ML), Bayes, and minimum mean squared error (MMSE) estimation.

When the maximum a posteriori probability (MAP)-based method is adopted to estimate TSC, the estimated TSC at the k -th radar pulse can be expressed as

$$\hat{\mathbf{g}}_{T,k} = \arg \max_{\mathbf{g}_{T,k}} p(\mathbf{g}_{T,k} | \mathbf{y}_k), \quad (4)$$

where $p(\mathbf{g}_{T,k} | \mathbf{y}_k)$ denotes the conditional probability distribution of $\mathbf{g}_{T,k}$ given the received waveform \mathbf{y}_k . To obtain the expression of MAP estimation explicitly, the MAP estimation can be simplified by the complex Gaussian distribution of \mathbf{y}_k given the TSC $\mathbf{g}_{T,k}$ with the complex Gaussian distribution. A function $G_{\mathbf{x}}(\boldsymbol{\mu}, \mathbf{R})$ is used to describe the complex Gaussian distribution of the vector $\mathbf{x} \sim \mathcal{CN}(\boldsymbol{\mu}, \mathbf{R})$, and $G_{\mathbf{x}}(\boldsymbol{\mu}, \mathbf{R})$ is

defined as $G_{\mathbf{x}}(\boldsymbol{\mu}, \mathbf{R}) \triangleq (2\pi)^{-M} \det(\mathbf{R})^{-1/2} e^{-1/2(\mathbf{x}-\boldsymbol{\mu})^H \mathbf{R}^{-1}(\mathbf{x}-\boldsymbol{\mu})}$, where M denotes the length of vector \mathbf{x} . Then, the MAP can be written as

$$\begin{aligned} \hat{\mathbf{g}}_{T,k} &= \arg \max_{\mathbf{g}_{T,k}} p(\mathbf{g}_{T,k}) p(\mathbf{y}_k | \mathbf{g}_{T,k}) \\ &= \arg \max_{\mathbf{g}_{T,k}} G_{\mathbf{g}_{T,k}}(\mathbf{0}, \mathbf{R}_T) G_{\mathbf{y}_k}(\mathbf{Z}_k \mathbf{g}_{T,k}, \mathbf{R}_{CN}), \end{aligned} \quad (5)$$

where $\mathbf{R}_{CN} \triangleq \mathbf{Z}_k \mathbf{R}_C \mathbf{Z}_k^H + \mathbf{R}_N$. After some simplifications, the estimated TSC at the k -th pulse using the MAP estimator can be represented as

$$\hat{\mathbf{g}}_{T,k} = \mathbf{Q}_k \mathbf{y}_k, \quad (6)$$

where the receiving filter of the MAP estimation is defined as

$$\mathbf{Q}_k \triangleq (\mathbf{Z}_k^H \mathbf{R}_{CN}^{-1} \mathbf{Z}_k + \mathbf{R}_T^{-1})^{-1} \mathbf{Z}_k^H \mathbf{R}_{CN}^{-1}. \quad (7)$$

Note that \mathbf{R}_{CN} can be rewritten as \mathbf{R}_N in the scenario without clutter [10], [11].

To exploit the temporal correlation of the extended target, a method based on KF is now proposed to estimate the TSC in the frequency domain, where the scenarios both with and without clutter are considered. For the initial step of KF estimation, the pulse index k is set to be 1, and the TSC can be estimated by the MAP estimator during the first pulse interval as

$$\hat{\mathbf{g}}_{T,1} = \mathbf{Q}_1 \mathbf{y}_1. \quad (8)$$

The estimation error can be measured by the MSE matrix. When the MAP-based method is used at the first step ($k = 1$) of the KF estimation, the initial MSE matrix can be calculated by

$$\begin{aligned} \mathbf{P}_{1|1} &= \mathcal{E} \left\{ (\hat{\mathbf{g}}_{T,1} - \mathbf{g}_{T,1}) (\hat{\mathbf{g}}_{T,1} - \mathbf{g}_{T,1})^H \right\} \\ &= \mathbf{Q}_1 (\mathbf{Z}_1 \mathbf{R}_T \mathbf{Z}_1^H + \mathbf{R}_{CN}) \mathbf{Q}_1^H - \mathbf{Q}_1 \mathbf{Z}_1 \mathbf{R}_T \\ &\quad - \mathbf{R}_T \mathbf{Z}_1^H \mathbf{Q}_1^H + \mathbf{R}_T. \end{aligned} \quad (9)$$

Then, we iteratively perform the following procedures for $k = 2, 3, \dots$, in Algorithm 1. In the KF estimation, the transmitted waveform can be optimized according to Section III. In

Algorithm 1: The KF-Based Method to Estimate TSC.

-
- 1: *Input:* received signal \mathbf{y}_k , maximum number of pulse K .
 - 2: *Initialization:* obtain $\hat{\mathbf{g}}_{T,1}$ from (6), and obtain $\mathbf{P}_{1|1}$ from (9).
 - 3: **for** $k = 2$ to K **do**
 - 4: $\hat{\mathbf{g}}_{T,k|k-1} = e^{-T_r/\tau} \hat{\mathbf{g}}_{T,k-1|k-1}$.
 - 5: $\mathbf{P}_{k|k-1} = e^{-2T_r/\tau} \mathbf{P}_{k-1|k-1} + (1 - e^{-2T_r/\tau}) \mathbf{R}_T$.
 - 6: $\hat{\mathbf{g}}_{T,k} = \mathbf{Q}_k \mathbf{y}_k$.
 - 7: $\Phi_k \triangleq \mathbf{P}_{k|k-1} \mathbf{Z}_k^H (\mathbf{Q}_k \mathbf{R}_{CN} + \mathbf{Q}_k \mathbf{Z}_k \mathbf{P}_{k|k-1} \mathbf{Z}_k^H)^{-1}$.
 - 8: $\hat{\mathbf{g}}_{T,k|k} = \hat{\mathbf{g}}_{T,k|k-1} + \Phi_k (\hat{\mathbf{g}}_{T,k} - \mathbf{Q}_k \mathbf{Z}_k \hat{\mathbf{g}}_{T,k|k-1})$.
 - 9: $\mathbf{P}_{k|k} = \mathbf{P}_{k|k-1} - \Phi_k \mathbf{Q}_k \mathbf{Z}_k \mathbf{P}_{k|k-1}$.
 - 10: Optimize the radar waveform \mathbf{s}_k using the method proposed in the following Section III.
 - 11: **end for**
 - 12: *Output:* the estimated TSC $\hat{\mathbf{g}}_{T,k|k}$.
-

the following section, the waveform optimization method subject to the constraints of transmitted energy, PAPR and detection probability will be given to improve the KF estimation performance.

III. OPTIMIZATION OF THE TRANSMITTED WAVEFORM

During the k -th iteration, the TSC estimation performance of the KF-based method can be measured by the trace of MSE matrix in Step 1 of Algorithm 1, i.e., $f(\mathbf{s}_k) = \text{Tr}\{\mathbf{P}_{k|k}\}$. In this paper, the transmitted waveform \mathbf{s}_k is optimized to minimize the estimation error $f(\mathbf{s}_k)$, and then to improve the estimation performance. During the waveform optimization processes, both the transmitted energy and PAPR constraints are considered to maximize the efficiency of the power amplifier. Since the target estimation relies on the presence of target, the target detection performance must be also considered. Therefore, an optimization problem subject to the constraints of transmitted energy, PAPR, and the target detection performance can be obtained during the k -th pulse

$$\begin{aligned}
 & \min_{\mathbf{s}_k} f(\mathbf{s}_k) \\
 & \text{s.t. } \|\mathbf{s}_k\|_2^2 \leq E_s \\
 & \quad \text{PAPR}(\mathbf{s}_k) \leq \zeta \\
 & \quad P_d(P_{fa}) \geq \epsilon.
 \end{aligned} \tag{10}$$

In the above optimization problem, E_s denotes the transmitted energy constraint, $\text{PAPR}(\mathbf{s}_k) \leq \zeta$ denotes the PAPR constraint to control the power dynamics, and $P_d(P_{fa}) \geq \epsilon$ denotes the detection probability constraint using a CFAR detector, where P_d and P_{fa} denote the detection probability and the false alarm rate, respectively.

To solve the waveform optimization problem (10), the objective function and constraints will be given explicitly and simplified. First, the objective function $f(\mathbf{s}_k)$ in (10) can be

written as

$$\begin{aligned}
 f(\mathbf{s}_k) & \stackrel{(a)}{=} \text{Tr}\{\mathbf{P}_{k|k-1} - \Phi_k \mathbf{Q}_k \mathbf{Z}_k \mathbf{P}_{k|k-1}\} \\
 & \stackrel{(b)}{=} \text{Tr}\left\{\mathbf{P}_{k|k-1} - \mathbf{P}_{k|k-1} \mathbf{Z}_k^H \mathbf{Q}_k^H (\mathbf{Q}_k \mathbf{R}_{CN} \mathbf{Q}_k^H \right. \\
 & \quad \left. + \mathbf{Q}_k \mathbf{Z}_k \mathbf{P}_{k|k-1} \mathbf{Z}_k^H \mathbf{Q}_k^H)^{-1} \mathbf{Q}_k \mathbf{Z}_k \mathbf{P}_{k|k-1}\right\} \\
 & \stackrel{(c)}{=} \text{Tr}\left\{\left(\mathbf{P}_{k|k-1}^{-1} + \mathbf{R}_C^{-1} - \right. \right. \\
 & \quad \left. \left. (\mathbf{R}_C + \mathbf{R}_C \mathbf{Z}_k^H \mathbf{R}_N^{-1} \mathbf{Z}_k \mathbf{R}_C)^{-1}\right)^{-1}\right\}. \tag{11}
 \end{aligned}$$

In (11), the equation (a) is obtained based on (9), the equation (b) is obtained by substituting Step 1 in Algorithm 1 into (a), and the equation (c) is obtained by the Woodbury identity¹ [35]. In the practical radar systems, the classical methods of parameter estimation can be used to estimate the parameter τ . Since this parameter estimation does not have any effect on the waveform optimization, so the estimation processes for the parameter τ have been ignored in this paper.

Then, the constraints in (10) will be simplified as follows. PAPR is defined as

$$\text{PAPR}(\mathbf{s}_k) \triangleq 10 \log_{10} \left(M \frac{\max_{1 \leq m \leq M} |s_{k,m}|^2}{\mathbf{s}_k^H \mathbf{s}_k} \right), \tag{12}$$

where M denotes the length of waveform \mathbf{s}_k , and $s_{k,m}$ denotes the m -th entry of \mathbf{s}_k . Therefore, the PAPR constraint can be rewritten as

$$\max_{1 \leq m \leq M} |s_{k,m}|^2 \leq 10^{\zeta/10} E_s / M \triangleq \zeta' E_s. \tag{13}$$

Next, the constraint of the target detection probability will be calculated and simplified. In the target detection problem, the echo signal can be written as

$$\begin{aligned}
 H_1: \mathbf{y}_k &= \mathbf{Z}_k (\mathbf{g}_{T,k} + \mathbf{g}_C) + \mathbf{w}, \\
 H_0: \mathbf{y}_k &= \mathbf{Z}_k \mathbf{g}_C + \mathbf{w},
 \end{aligned} \tag{14}$$

where H_1 and H_0 denote the presence and absence of target, respectively. According to the estimated TSC $\hat{\mathbf{g}}_{T,k}$, the distribution of echo signal is

$$\begin{aligned}
 \mathbf{y}_k | H_0 & \sim \mathcal{CN}\{\mathbf{0}, \mathbf{R}_{CN}\}, \\
 \mathbf{y}_k | H_1 & \sim \mathcal{CN}\{\mathbf{Z}_k \hat{\mathbf{g}}_{T,k}, \mathbf{R}_{CN}\}.
 \end{aligned} \tag{15}$$

When a likelihood ratio test is used to detect the target, we have

$$\frac{p(\mathbf{y}_k | H_1)}{p(\mathbf{y}_k | H_0)} = \frac{G_{\mathbf{y}_k}(\mathbf{Z}_k \hat{\mathbf{g}}_{T,k}, \mathbf{R}_{CN})}{G_{\mathbf{y}_k}(\mathbf{0}, \mathbf{R}_{CN})} \stackrel{H_1}{\geq} \theta, \tag{16}$$

where θ denotes the detection threshold. After some simplifications, the target detection problem can be written as

$$d(\mathbf{y}_k) \triangleq \mathbf{y}_k^H \mathbf{R}_{CN}^{-1} \mathbf{Z}_k \hat{\mathbf{g}}_{T,k} \stackrel{H_1}{\underset{H_0}{\geq}} \theta. \tag{17}$$

¹ $(\mathbf{A} + \mathbf{C} \mathbf{B} \mathbf{C}^H)^{-1} = \mathbf{A}^{-1} - \mathbf{A}^{-1} \mathbf{C} (\mathbf{B}^{-1} + \mathbf{D} \mathbf{C})^{-1} \mathbf{D}$, where $\mathbf{D} \triangleq \mathbf{C}^H \mathbf{A}^{-1}$.

In the CFAR detector, the false alarm rate is calculated by

$$\begin{aligned} P_{fa} &\triangleq p(d(\mathbf{y}_k) > \theta | H_0) \\ &= Q\left(\theta / \sqrt{(\mathbf{Z}_k \hat{\mathbf{g}}_{T,k})^H \mathbf{R}_{CN}^{-1} \mathbf{Z}_k \hat{\mathbf{g}}_{T,k}}\right), \end{aligned} \quad (18)$$

where the Q function is defined as $Q(x) \triangleq \frac{1}{\sqrt{2\pi}} \int_x^\infty \exp(-\mu^2/2) d\mu$. Thus, the threshold of the CFAR detection in (17) can be obtained as

$$\theta(P_{fa}) = Q^{-1}(P_{fa}) \sqrt{(\mathbf{Z}_k \hat{\mathbf{g}}_{T,k})^H \mathbf{R}_{CN}^{-1} \mathbf{Z}_k \hat{\mathbf{g}}_{T,k}}. \quad (19)$$

Therefore, the detection probability with the false alarm rate P_{fa} is

$$\begin{aligned} P_d(P_{fa}) &\triangleq p(d(\mathbf{y}_k) > \theta(P_{fa}) | H_1) \\ &= Q\left(Q^{-1}(P_{fa}) - \sqrt{(\mathbf{Z}_k \hat{\mathbf{g}}_{T,k})^H \mathbf{R}_{CN}^{-1} \mathbf{Z}_k \hat{\mathbf{g}}_{T,k}}\right). \end{aligned} \quad (20)$$

Since $Q(\cdot)$ is a monotone decreasing function, the detection probability constraint in (10) based on (20) can be written as

$$\mathbf{z}_k^H \hat{\mathbf{G}}_k^H \mathbf{R}_{CN}^{-1} \hat{\mathbf{G}}_k \mathbf{z}_k \geq \epsilon' \quad (21)$$

where $\hat{\mathbf{G}}_k \triangleq \text{diag}\{\hat{\mathbf{g}}_{T,k}\}$, and $\epsilon' \triangleq (Q^{-1}(P_{fa}) - Q^{-1}(\epsilon))^2$.

Now, with the simplified objective function and constraints, the explicit formula of the optimization problem (10) can be obtained as

$$\begin{aligned} \min_{\mathbf{s}_k} &\left\{ \text{Tr} \left[\left(\mathbf{P}_{k|k-1}^{-1} + \mathbf{R}_C^{-1} \right. \right. \right. \\ &\quad \left. \left. \left. - \left(\mathbf{R}_C + \mathbf{R}_C \mathbf{Z}_k^H \mathbf{R}_N^{-1} \mathbf{Z}_k \mathbf{R}_C \right)^{-1} \right)^{-1} \right] \right\} \\ \text{s.t.} &\quad \|\mathbf{s}_k\|_2^2 \leq E_s \\ &\quad \max_{1 \leq m \leq M} |s_{k,m}|^2 \leq \xi' E_s \\ &\quad \mathbf{z}_k^H \hat{\mathbf{G}}_k^H \mathbf{R}_{CN}^{-1} \hat{\mathbf{G}}_k \mathbf{z}_k \geq \epsilon'. \end{aligned} \quad (22)$$

However, this optimization problem is non-convex, and cannot be solved efficiently [36], [37]. Thus, we propose a novel two-step method to convert the original non-convex problem into several convex ones, which can be solved efficiently.

IV. TWO-STEP METHOD

Different from the existing indirect methods, a two-step direct method is proposed in this paper to solve the non-convex optimization problem in (22). As shown in Fig. 2, for the first step, an initial radar waveform regardless of clutter is obtained by relaxing the original problem into a convex SDP problem. For the second step, an iterative method is proposed to obtain a term and update the initial radar waveform obtained from the first step, so that a solution of the original non-convex problem (22) can be obtained. The SDP problem can be solved efficiently by the optimization toolboxes, such as CVX [38], [39].

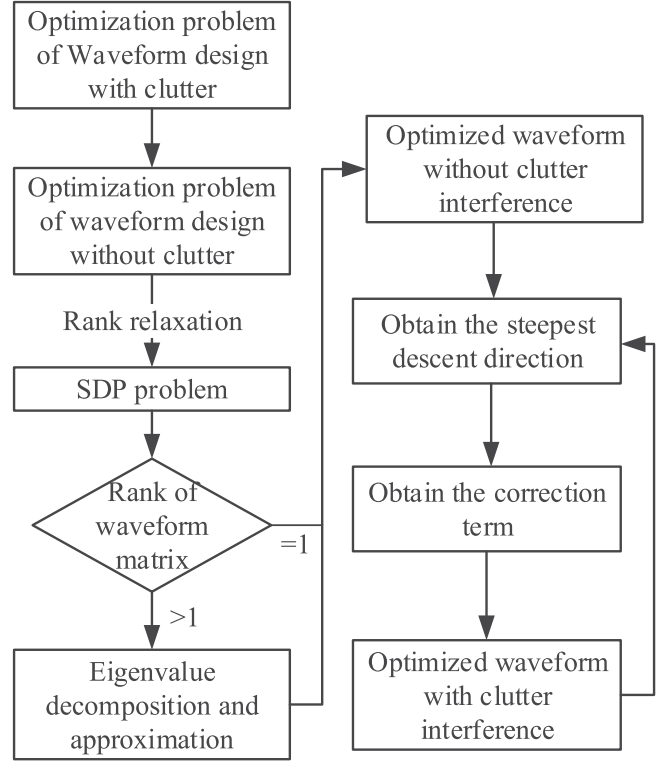


Fig. 2. The flowchart of the two-step method to optimize the transmitted waveform in the scenario with clutter and noise.

Algorithm 2: Waveform Optimization Without Clutter.

- 1: Define $\mathbf{W}_k \triangleq \mathbf{s}_k \mathbf{s}_k^H$ and $\mathbf{W}_k \succeq 0$.
 - 2: Convert the non-convex problem (23) for the scenario without clutter into a convex problem (24).
 - 3: Obtain \mathbf{W}_k^* from (24).
 - 4: **if** $\text{rank}\{\mathbf{W}_k^*\} = 1$ **then**
 - 5: The optimized waveform without clutter $\bar{\mathbf{s}}_k$ can be obtained by the decomposition $\mathbf{W}_k^* = \bar{\mathbf{s}}_k \bar{\mathbf{s}}_k^H$.
 - 6: **else**
 - 7: $\mathbf{W}_k^* = \sum_i \lambda_i \mathbf{v}_i \mathbf{v}_i^H$. Denote \mathbf{v}_{\max} as the eigenvector corresponding to the largest eigenvalue λ_{\max} .
 - 8: Obtain $\bar{\mathbf{s}}_k$ from the optimization problem (32) with \mathbf{v}_{\max} .
 - 9: **end if**
 - 10: **Output:** the optimized waveform $\bar{\mathbf{s}}_k$.
-

A. Waveform Design Regardless of Clutter

The waveform optimization method in the scenario without clutter is described in Algorithm 2, and more details are given as follows.

Regardless of clutter which is essentially to set $\mathbf{R}_{CN} = \mathbf{R}_N$ in (11) and (17), the non-convex optimization problem in (22) can be written as

$$\begin{aligned} \min_{\mathbf{s}_k} &\left\{ \text{Tr} \left[\left(\mathbf{P}_{k|k-1}^{-1} + \mathbf{Z}_k^H \mathbf{R}_N^{-1} \mathbf{Z}_k \right)^{-1} \right] \right\} \\ \text{s.t.} &\quad \|\mathbf{s}_k\|_2^2 \leq E_s \end{aligned}$$

$$\begin{aligned} & \max_{1 \leq m \leq M} |s_{k,m}|^2 \leq \xi' E_s \\ & \mathbf{s}_k^H \mathbf{F}^H \hat{\mathbf{G}}_k^H \mathbf{R}_N^{-1} \hat{\mathbf{G}}_k \mathbf{F} \mathbf{s}_k \geq \epsilon', \end{aligned} \quad (23)$$

where the covariance matrix of noise \mathbf{R}_N can be estimated from the secondary data having the same properties with the primary data [6], [40]. With the definition of a semidefinite matrix $\mathbf{W}_k \triangleq \mathbf{s}_k \mathbf{s}_k^H$, the optimization problem (23) can be rewritten as

$$\begin{aligned} & \min_{\mathbf{W}_k} \left\{ \text{Tr} \left[\left(\mathbf{P}_{k|k-1}^{-1} + \mathbf{F} \mathbf{W}_k \mathbf{F}^H \circ \mathbf{R}_N^{-1} \right)^{-1} \right] \right\} \\ & \text{s.t. } \text{Tr} \{ \mathbf{W}_k \} \leq E_s \\ & \text{diag} \{ \mathbf{W}_k \} \leq \xi' E_s \\ & \text{Tr} \left\{ \hat{\mathbf{G}}_k^H \mathbf{R}_N^{-1} \hat{\mathbf{G}}_k \mathbf{F} \mathbf{W}_k \mathbf{F}^H \right\} \geq \epsilon' \\ & \text{rank} \{ \mathbf{W}_k \} = 1 \\ & \mathbf{W}_k \succeq 0, \end{aligned} \quad (24)$$

where \circ denotes the Hadamard product. With the rank constraint $\text{rank}\{\mathbf{W}_k\} = 1$, the optimization problem (24) is non-convex, so a SDP problem [14] can be relaxed by removing the rank constraint as

$$\begin{aligned} & \min_{\mathbf{W}_k} \left\{ \text{Tr} \left[\left(\mathbf{P}_{k|k-1}^{-1} + \mathbf{F} \mathbf{W}_k \mathbf{F}^H \circ \mathbf{R}_N^{-1} \right)^{-1} \right] \right\} \\ & \text{s.t. } \text{Tr} \{ \mathbf{W}_k \} \leq E_s \\ & \text{diag} \{ \mathbf{W}_k \} \leq \xi' E_s \\ & \text{Tr} \left\{ \hat{\mathbf{G}}_k^H \mathbf{R}_N^{-1} \hat{\mathbf{G}}_k \mathbf{F} \mathbf{W}_k \mathbf{F}^H \right\} \geq \epsilon' \\ & \mathbf{W}_k \succeq 0, \end{aligned} \quad (25)$$

which is convex and can be solved efficiently by the optimization toolbox, such as CVX. The solution of the SDP problem (25) is denoted \mathbf{W}_k^* .

If $\text{rank}\{\mathbf{W}_k^*\} = 1$, then \mathbf{W}_k^* is a solution of (24), meanwhile the corresponding solution of (23) can be obtained via the decomposition $\mathbf{W}_k^* = \bar{\mathbf{s}}_k \bar{\mathbf{s}}_k^H$, where $\bar{\mathbf{s}}_k$ denotes the optimized waveform without clutter.

Otherwise, if $\text{rank}\{\mathbf{W}_k^*\} > 1$, \mathbf{W}_k^* has the following eigenvalue decomposition $\mathbf{W}_k^* = \sum_{i=1}^r \lambda_i \mathbf{v}_i \mathbf{v}_i^H$, where r denotes the number of nonzero eigenvalues, λ_i denotes the i -th eigenvalue, and \mathbf{v}_i denotes the corresponding eigenvector. Then, the eigenvector corresponding to the maximal eigenvalue $|\lambda_{\max}|$ of \mathbf{W}_k^* is \mathbf{v}_{\max} . Since $\lambda_{\max} \mathbf{v}_{\max} \mathbf{v}_{\max}^H$ can be used to approximate the waveform matrix \mathbf{W}_k^* by [14]

$$\mathbf{W}_k^* \approx \lambda_{\max} \mathbf{v}_{\max} \mathbf{v}_{\max}^H, \quad (26)$$

the energy normalized vector $\sqrt{E_s} \mathbf{v}_{\max} / \|\mathbf{v}_{\max}\|_2$ can be used to approximate the optimized waveform $\bar{\mathbf{s}}_k$ at the k -th pulse without clutter.

However, the eigenvector approximation does not satisfy the constraints in the optimization problem (23), so the transmitted waveform must satisfy the constraints and also approach the eigenvector \mathbf{v}_{\max} . Additionally, considering that the constraint of the target detection probability in (23) is non-convex, we

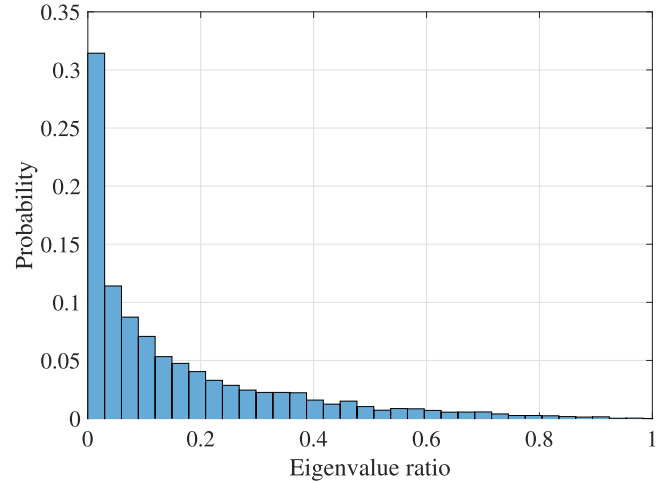


Fig. 3. The eigenvalue ratio probability of the matrix \mathbf{U} .

define

$$\mathbf{U} \triangleq \mathbf{F}^H \hat{\mathbf{G}}_k^H \mathbf{R}_N^{-1} \hat{\mathbf{G}}_k \mathbf{F}. \quad (27)$$

In Fig. 3, we show the probability of the eigenvalue ratio $r \triangleq |\theta'|/|\theta_{\max}|$, where θ_{\max} and θ' denote the largest and second largest eigenvalues, respectively. The eigenvalue ratios are obtained by realizing the matrix \mathbf{U} according to the different types of target and noise, where the entries of both \mathbf{R}_T and \mathbf{R}_N follow the uniform distribution. Since the largest eigenvalue is much larger than the others with high probability, the matrix \mathbf{U} can be approximated using the maximum eigenvalue decomposition

$$\mathbf{U} \approx \theta_{\max} \mathbf{w}_{\max} \mathbf{w}_{\max}^H, \quad (28)$$

where \mathbf{w}_{\max} denotes the eigenvector of \mathbf{U} corresponding to the largest eigenvalue θ_{\max} . Then, the constraint of the target detection probability can be approximated by

$$\mathbf{s}_k^H \mathbf{U} \mathbf{s}_k \approx \mathbf{s}_k^H \theta_{\max} \mathbf{w}_{\max} \mathbf{w}_{\max}^H \mathbf{s}_k \geq \epsilon'. \quad (29)$$

Therefore, the target detection constraint can be rewritten as

$$|\mathbf{s}_k^H \mathbf{w}_{\max}|^2 \geq \epsilon' / \theta_{\max}. \quad (30)$$

Then, a more strict constraint can be used in the optimization problem (24) as the detection constraint

$$\mathcal{R} \{ \mathbf{s}_k^H \mathbf{w}_{\max} \} \geq \sqrt{\epsilon' / \theta_{\max}}, \quad (31)$$

which is affine and convex.

If $\text{rank}\{\mathbf{W}_k^*\} > 1$, the optimized waveform $\bar{\mathbf{s}}_k$ for the scenario without clutter can be obtained by the following convex optimization problem

$$\begin{aligned} & \min_{\mathbf{s}_k} \left(-\mathbf{s}_k^H \mathbf{v}_{\max} \right) \\ & \text{s.t. } \|\mathbf{s}_k\|_2^2 \leq E_s \\ & \max_{1 \leq m \leq M} |s_{k,m}|^2 \leq \xi' E_s \\ & \mathcal{R} \{ \mathbf{s}_k^H \mathbf{w}_{\max} \} \geq \sqrt{\epsilon' / \theta_{\max}}, \end{aligned} \quad (32)$$

Algorithm 3: The Method to Obtain the Correction Term and Fix the Optimized Waveform.

- 1: *Input:* optimized waveform $\bar{\mathbf{s}}_k$ for the scenario without clutter, minimum coefficient ϵ_α , maximum number of iterations J .
 - 2: *Initialization:* correction term $\mathbf{a}_{k,0}^* = \mathbf{0}$, corrected waveform $\bar{\mathbf{s}}_k$ as $\mathbf{s}_{k,0}^* = \bar{\mathbf{s}}_k + \mathbf{a}_{k,0}^*$, correction coefficient $\alpha = 1$.
 - 3: **for** $j = 1$ to J **do**
 - 4: With the transmitted waveform $\mathbf{s}_{k,j}^*$, obtain the steepest descent direction $\mathbf{d}_{k,j}$ from (33).
 - 5: Obtain the correction term $\mathbf{a}_{k,j}^*$ from (44).
 - 6: $\mathbf{s}_{k,j}^* = \mathbf{s}_{k,j-1}^* + \mathbf{a}_{k,j}^*$ ($\|\mathbf{a}_{k,j}^*\|_2^2 \leq \alpha E_s$).
 - 7: **if** $f(\mathbf{s}_{k,j}^*) \leq f(\mathbf{s}_{k,j-1}^*)$ **then**
 - 8: $\alpha = \alpha/2$.
 - 9: **end if**
 - 10: **if** $\alpha \leq \epsilon_\alpha$ **then**
 - 11: **break.**
 - 12: **end if**
 - 13: **end for**
 - 14: *Output:* the optimized waveform $\mathbf{s}_{k,j}^*$ for the k -th KF estimation.
-

where the objective function is the simplified result of the angle between \mathbf{s}_k and \mathbf{v}_{\max} . Since \mathbf{v}_{\max} is normalized, the optimized waveform \mathbf{s}_k satisfies $\|\mathbf{s}_k\|_2^2 = E_s$.

B. Waveform Design Regarding Clutter

Based on the previous subsection, the optimized waveform $\bar{\mathbf{s}}_k$ in the scenario without clutter has been obtained. With the presence of clutter, an iterative method is proposed to obtain a correction term \mathbf{a}_k , which can fix the initially optimal waveform $\bar{\mathbf{s}}_k$, and the optimized waveform \mathbf{s}_k^* can be achieved as the solution of (22). The iterative method to obtain the correction term is described in Algorithm 3, and more details are given as follows.

The steepest descent direction $\mathbf{d}_{k,j}$ at Step 3 of Algorithm 3 can be obtained by the following convex optimization problem

$$\begin{aligned}
 & \mathbf{d}_{k,j} = \arg \min_{\mathbf{d}} z \\
 & \text{s.t. } \nabla f(\mathbf{s}_{k,j}^*)^T \mathbf{d} \leq z \\
 & \quad \nabla g_i(\mathbf{s}_{k,j}^*)^T \mathbf{d} \leq z, i = 1, 2, 3 \\
 & \quad -1 \leq d_m \leq 1, m = 1, 2, \dots, M
 \end{aligned} \quad (33)$$

where the objective function $f(\mathbf{s}_{k,j}^*)$ with clutter is given in (11). We further define $g_i(\mathbf{s}_{k,j}^*)$ as

$$g_1(\mathbf{s}_{k,j}^*) \triangleq \|\mathbf{s}_{k,j}^*\|_2^2 - E_s \quad (34)$$

$$g_2(\mathbf{s}_{k,j}^*) \triangleq \xi' E_s - \max_{1 \leq m \leq M} |s_{k,j,m}^*|^2 \quad (35)$$

$$g_3(\mathbf{s}_{k,j}^*) \triangleq \mathbf{s}_{k,j}^{*H} \mathbf{F}^H \hat{\mathbf{G}}_k^H \mathbf{R}_{CN}^{-1} \hat{\mathbf{G}}_k \mathbf{F} \mathbf{s}_{k,j}^* - \epsilon', \quad (36)$$

where $s_{k,j,m}^*$ is the m -th entry of $\mathbf{s}_{k,j}^*$.

The solution of problem (33) is the steepest descent direction [41], and the constraints $-1 \leq d_m \leq 1$ are adopted to guarantee a finite optimal direction. Therefore, the derivation of objective function $\nabla f(\mathbf{s}_{k,j}^*)$ is given in (37), shown at the bottom of this page, where $\mathbf{z}_{k,j}^* \triangleq \mathbf{F} \mathbf{s}_{k,j}^*$, $\mathbf{Z}_{k,j}^* \triangleq \text{diag}\{\mathbf{z}_{k,j}^*\}$, $z_{k,j,m}^*$ is the m -th entry of $\mathbf{z}_{k,j}^*$, Δ_{mn} is a zero matrix except the entry at the m -th row and n -th column being 1, and the matrix \mathbf{X} is defined as

$$\mathbf{X} \triangleq \mathbf{P}_{k|k-1}^{-1} + \mathbf{R}_C^{-1} - (\mathbf{R}_C + \mathbf{R}_C \mathbf{Z}_{k,j}^{*H} \mathbf{R}_N^{-1} \mathbf{Z}_{k,j}^* \mathbf{R}_C)^{-1}. \quad (38)$$

Thus, we have

$$\nabla f(\mathbf{s}_{k,j}^*) = \left(\frac{\partial f(\mathbf{s}_{k,j}^*)}{\partial z_{k,j,1}^*}, \frac{\partial f(\mathbf{s}_{k,j}^*)}{\partial z_{k,j,2}^*}, \dots, \frac{\partial f(\mathbf{s}_{k,j}^*)}{\partial z_{k,j,M}^*} \right) \mathbf{F}. \quad (39)$$

The derivations for the constraints can be also obtained as

$$\nabla g_1(\mathbf{s}_{k,j}^*) = \frac{\partial g_1(\mathbf{s}_{k,j}^*)}{\partial \mathbf{s}_{k,j}^*} = 2\mathbf{s}_{k,j}^*, \quad (40)$$

$$\nabla g_2(\mathbf{s}_{k,j}^*) = \frac{\partial g_2(\mathbf{s}_{k,j}^*)}{\partial \mathbf{s}_{k,j}^*} = \mathbf{p}, \quad (41)$$

where the m^* -th entry of \mathbf{p} is $2|s_{k,j,m}^*|$ with $m^* = \arg \max_{1 \leq m \leq M} |s_{k,j,m}^*|^2$, and the rest entries are zeros. Additionally, $\nabla g_3(\mathbf{s}_{k,j}^*)$ can be approximated by

$$\nabla g_3(\mathbf{s}_{k,j}^*) = \frac{\partial g_3(\mathbf{s}_{k,j}^*)}{\partial \mathbf{s}_{k,j}^*} \approx \mathbf{g}', \quad (42)$$

where the m -th entry of \mathbf{g}' can be obtained as

$$\mathbf{g}'_m \triangleq \frac{g_3(\mathbf{s}_{k,j}^* + \delta_{g,m}) - g_3(\mathbf{s}_{k,j}^*)}{\|\delta_{g,m}\|_2}, \quad (43)$$

and $\delta_{g,m}$ is a vector with the m -th entry being $0 < \delta_g \ll 1$ and other entries being zeros.

$$\begin{aligned}
 \frac{\partial f(\mathbf{s}_{k,j}^*)}{\partial z_{k,j,m}^*} &= -\text{Tr} \left\{ \mathbf{X}^{-2T} \frac{\partial (\mathbf{R}_C + \mathbf{R}_C \mathbf{Z}_{k,j}^{*H} \mathbf{R}_N^{-1} \mathbf{Z}_{k,j}^* \mathbf{R}_C)^{-1}}{\partial z_{k,j,m}^*} \right\} \\
 &= \text{Tr} \left\{ \mathbf{X}^{-2T} (\mathbf{I} + \mathbf{Z}_{k,j}^{*H} \mathbf{R}_N^{-1} \mathbf{Z}_{k,j}^* \mathbf{R}_C)^{-1} (\Delta_{mm} \mathbf{R}_N^{-1} \mathbf{Z}_{k,j}^* + \mathbf{Z}_{k,j}^{*H} \mathbf{R}_N^{-1} \Delta_{mm}) (\mathbf{I} + \mathbf{R}_C \mathbf{Z}_{k,j}^{*H} \mathbf{R}_N^{-1} \mathbf{Z}_{k,j}^*) \right\} \quad (37)
 \end{aligned}$$

At Step 5 of Algorithm 3, the correction term $\mathbf{a}_{k,j}^*$ can be calculated by maximizing the correlation with the steepest descent direction $\mathbf{d}_{k,j}$. Then, the following optimization problem can be obtained

$$\begin{aligned} \mathbf{a}_{k,j}^* &= \arg \min_{\mathbf{a}} \left(-\mathbf{a}_k^H \mathbf{d}_{k,j} \right) \\ \text{s.t. } \|\mathbf{a}\|_2^2 &\leq \alpha E_s \\ \mathbf{s}' &= \mathbf{s}_{k,j-1}^* + \mathbf{a} \\ \|\mathbf{s}'\|_2^2 - E_s &\leq 0 \\ \xi' E_s - \max_{1 \leq m \leq M} |s'_m|^2 &\geq 0 \\ \mathcal{R} \left\{ \mathbf{s}'^H \mathbf{w}_{\max} \right\} - \sqrt{\epsilon' / \theta_{\max}} &\geq 0, \end{aligned} \quad (44)$$

where the normalized $\mathbf{d}_{k,j}$ and the optimized $\mathbf{a}_{k,j}^*$ with $\|\mathbf{a}_{k,j}^*\|_2^2 = \alpha E_s$ simplify the objective function from the angle between \mathbf{a}_k and $\mathbf{d}_{k,j}$ to $(-\mathbf{a}_k^H \mathbf{d}_{k,j})$.

Finally, the optimized waveform can be obtained as $\mathbf{s}_{k,j-1}^* + \mathbf{a}_{k,j}^*$, and the convergence of the proposed iterative method to iteratively fix the waveform $\mathbf{s}_{k,j-1}^*$ by an optimized correction term $\mathbf{a}_{k,j}^*$ will be given in the following simulation section.

C. Complexity Analysis

When an interior-point algorithm is adopted to solve the SDP problem (25), the computational complexity is roughly $\mathcal{O}(M^{4.5})$ [42]. Additionally, since both (32) and (33) are the linear programming problems, both the computational complexities are $\mathcal{O}(M^3 / \log M)$ [43]. Therefore, the totally computational complexity of the proposed two-step method can be roughly obtained as $\mathcal{O}(M^{4.5} + 2M^3 / \log M)$.

D. Cramér-Rao Bound of the Estimated TSC

In the TSC estimation, the estimation performance is bounded by Cramér-Rao bound, so the Cramér-Rao bound will be given in this subsection. With the given transmitted waveform \mathbf{s}_k and TSC $\mathbf{g}_{T,k}$, the likelihood function of the received signal can be obtained as

$$p(\mathbf{y}_k | \mathbf{g}_{T,k}) = G_{\mathbf{y}_k}(\mathbf{Z}_k \mathbf{g}_{T,k}, \mathbf{R}_{CN}). \quad (45)$$

Therefore, we have

$$\frac{\partial \ln p(\mathbf{y}_k | \mathbf{g}_{T,k})}{\partial \mathbf{g}_{T,k}} = \mathbf{Z}_k^H \mathbf{R}_{CN}^{-1} (\mathbf{y}_k - \mathbf{Z}_k \mathbf{g}_{T,k}), \quad (46)$$

and the Fisher information matrix is

$$\begin{aligned} \mathbf{I}(\mathbf{g}_{T,k}) &\triangleq \mathbb{E} \left\{ \left(\frac{\partial \ln p(\mathbf{y}_k | \mathbf{g}_{T,k})}{\partial \mathbf{g}_{T,k}} \right) \left(\frac{\partial \ln p(\mathbf{y}_k | \mathbf{g}_{T,k})}{\partial \mathbf{g}_{T,k}} \right)^H \right\} \\ &= \mathbf{Z}_k^H (\mathbf{R}_{CN}^{-1})^H \mathbf{Z}_k. \end{aligned} \quad (47)$$

Therefore, the Cramér-Rao bound of the estimated TSC can be obtained as

$$\mathcal{B} \triangleq \mathbf{I}(\mathbf{g}_{T,k})^{-1} = \left[\mathbf{Z}_k^H (\mathbf{R}_{CN}^{-1})^H \mathbf{Z}_k \right]^{-1}. \quad (48)$$

TABLE I
SIMULATION PARAMETERS

Parameter	Value
The signal-to-noise ratio (SNR) of echo signal	-10 dB
The signal-to-clutter ratio (SCR) of echo signal	-15 dB
The pulse repetition interval (PRI)	1 ms
The pulse duration	0.1 ms
The sampling frequency	160 KHz
The temporal decay constant τ	1 s
The transmit energy E_s	1
The number of target realization	30
The pulse number	50
The waveform length	16
The preset P_d	0.95
The preset P_{f_a}	0.05
PAPR	3 dB

The variance of the estimated TSC is bounded by the Cramér-Rao bound, and for the i -th TSC $g_{T,k,i}$, we have $\text{var}(g_{T,k,i}) \geq \mathcal{B}_{i,i}$, where $\mathcal{B}_{i,i}$ is the i -th column and i -th row entry of \mathcal{B} .

V. SIMULATION RESULTS

In this section, the simulation results are shown, and the simulation parameters are given in Table I. The covariance matrices of both TSC and noise are chosen by the uniform random distribution, and the covariance matrices for running one realization are shown in Fig. 4.

In Fig. 5, the PAPR comparison of the optimized waveform with random waveforms is given. Since PAPR is one of the constraints for optimization, the optimized waveforms with or without clutter can achieve 3 dB PAPR. To make fair comparisons regarding estimation performance with the same PAPR constraint, only the random waveforms satisfying 3 dB PAPR are selected for the comparisons, as shown in Fig. 5. Therefore, all the transmitted waveforms used in our scenario satisfy the PAPR constraint. In Fig. 6, the PSD of an optimized waveform is given, and the PSDs of both target and clutter are also given. As shown in this figure, the optimized waveform transmits more energy in the spectrum with a relatively higher ratio between the target PSD and clutter PSD, so the SCNR of the received signal can be improved.

We simulate the TSC estimation in the scenario without clutter. As shown in Fig. 7, we show the estimation performance for different SNRs, where the KF estimator with both non-optimized [10], [11], [44] and optimized waveforms are adopted. The estimation performance is measured by the normalized MSE, which is defined as

$$q(\hat{\mathbf{g}}_{T,k}, \mathbf{g}_{T,k}) \triangleq \frac{\|\hat{\mathbf{g}}_{T,k} - \mathbf{g}_{T,k}\|_2^2}{\|\mathbf{g}_{T,k}\|_2^2}. \quad (49)$$

As shown in Fig. 7, the KF estimator works at SNR = -20 dB, -15 dB and -10 dB, respectively. By exploiting the temporal

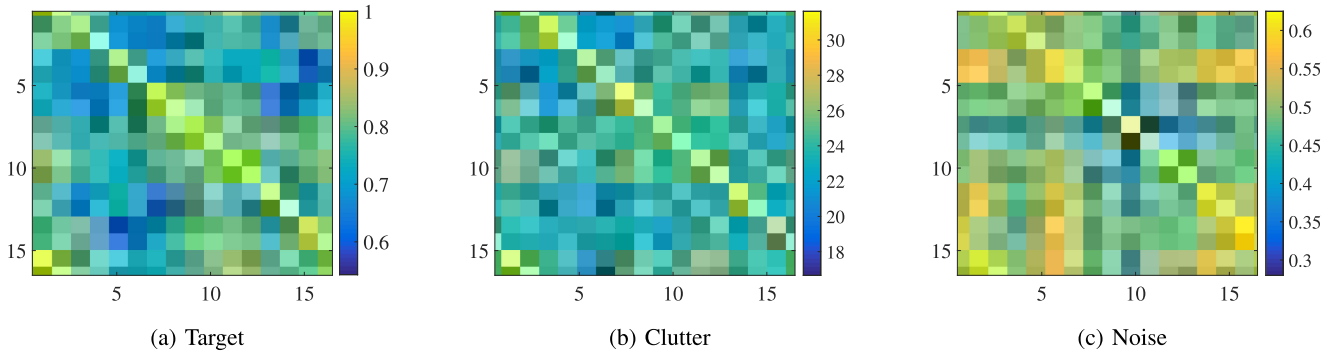


Fig. 4. The covariance matrices of the scattering coefficients and noise.

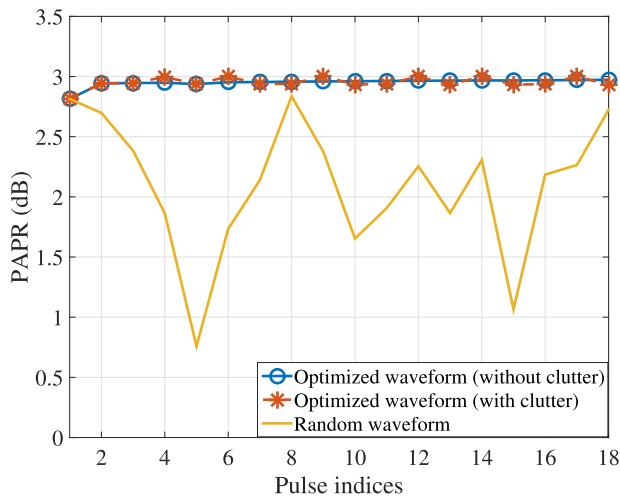


Fig. 5. The PAPR of transmitted waveforms.

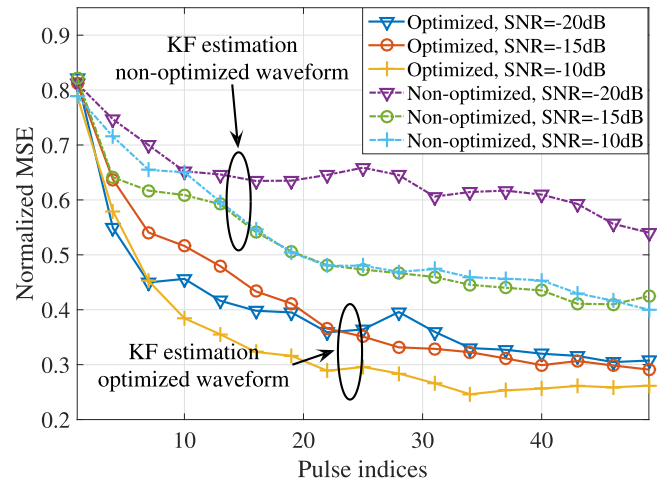


Fig. 7. KF estimation at different SNR without clutter.

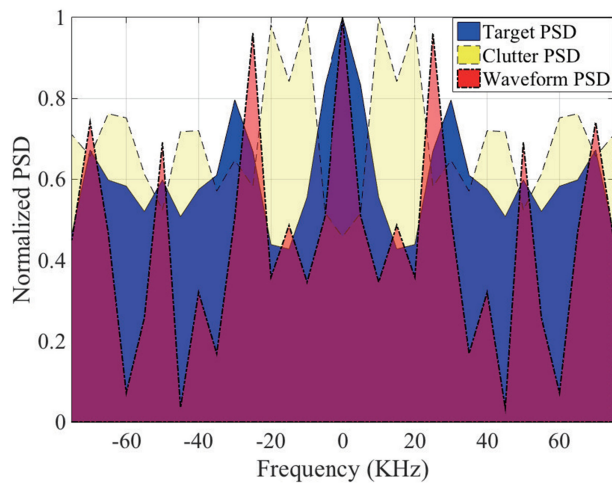


Fig. 6. The PSD of optimized waveform.

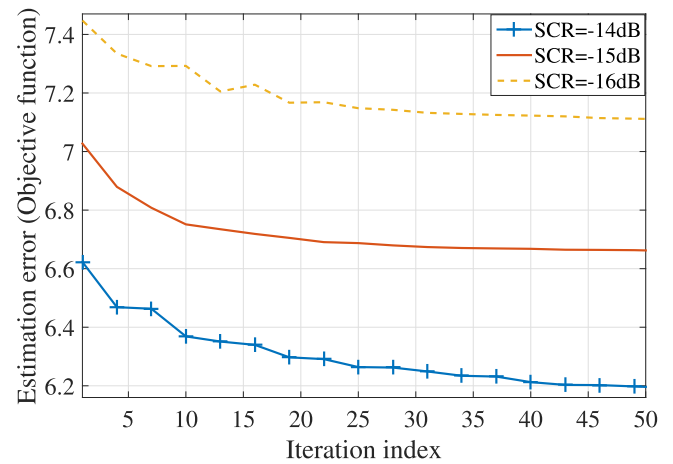


Fig. 8. Iteration error of correction term.

correlation, the KF estimator outperforms the single pulse based MAP estimator. The decreasing SNR reduces the KF estimation performance both with and without waveform optimization, but the proposed method of the waveform optimization still works well and outperforms the non-optimized waveform.

When we consider the waveform optimization in the scenario with clutter, the iterative method has been proposed to fix the optimized waveform in the scenario without clutter. The convergence of proposed iterative method is illustrated in Fig. 8 at SCR = -14 dB, -15 dB and -16 dB. The maximum number of iterations is set to be $J = 50$, and the minimum correction

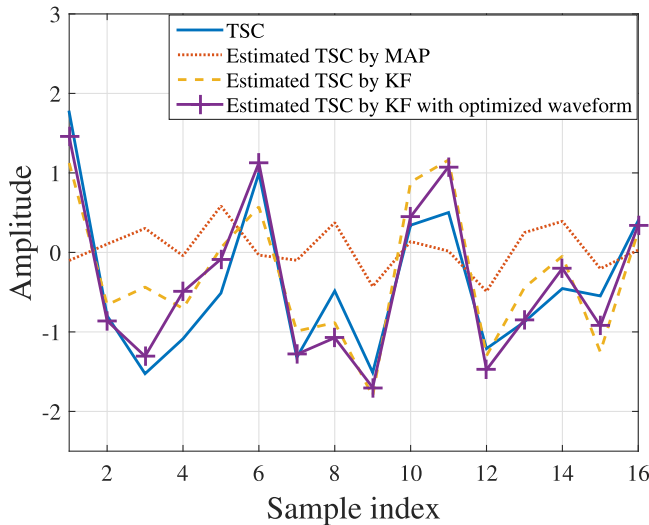


Fig. 9. The estimated TSC with different methods.

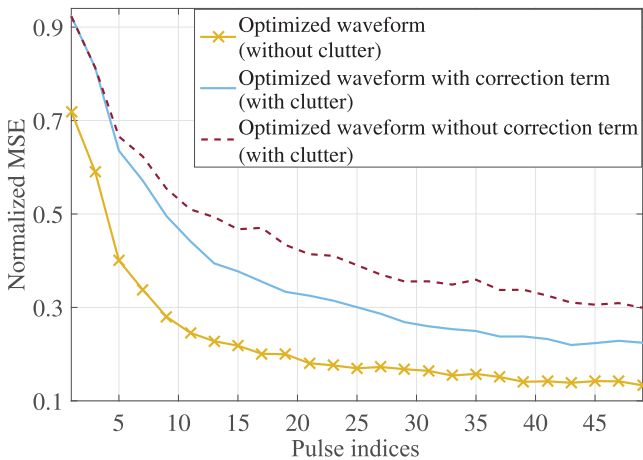


Fig. 10. TSC estimation performance of KF method.

coefficient is $\epsilon_\alpha = 10^{-4}$ in Algorithm 3. As shown in Fig. 8, when the iteration number is 50, the objective function in (11), which describes the KF estimation performance with clutter, converges to a steady state. This steady state has lower estimation error than the initially optimal waveform regardless of the clutter.

For the second step of the proposed waveform optimization method, the iterative method is used to fix the initially optimal waveform, so this operation must be able to eliminate the performance reduction caused by the clutter. We give the simulation results in Fig. 10, where the KF estimator is used. We first show the normalized MSE with the optimized waveform in the scenario without clutter, which has the best estimation performance. Then, the clutter is introduced, and the normalized MSE is improved from 0.17 to 0.37 at the 30-th pulse, where the same optimized waveform is utilized. By using the iterative method to fix this optimized waveform, the normalized MSE is

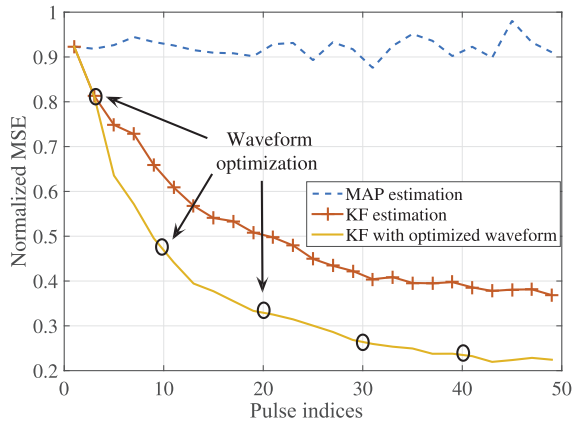
reduced to 0.25, so the clutter is eliminated by 32% using the additional correction term $\mathbf{a}_{k,j}^*$ in (44).

Then, in the scenario with clutter, we first show the estimated TSC with different methods in Fig. 9, where the simulation parameters are the same as Table I. As shown in this figure, the KF-based method with the optimized waveform achieves the best estimation performance. Additionally, to give a clear illustration, we also show the normalized MSE performance with different simulation parameters in Fig. 11, where the MAP estimator, the KF estimator and the KF estimator with optimized waveform are compared. In Fig. 11 a, we have SCR = -15 dB, SNR = -10 dB and $\tau = 1$ s. The KF estimation performance is improved by optimizing the transmitted waveform at the 3, 10, 20, 30, 40-th pulses. At the 30-th pulse, the normalized MSE is reduced by 35% using the optimized waveform in the KF estimator. Additionally, in Fig. 11 b, we randomly choose the covariance matrices of the scattering coefficients and noise at each simulation, and average the normalized MSE. The proposed estimation method also achieves the best performance. Then, since the lower correlation time τ reduces the KF estimation performance, we reduce the correlation time to $\tau = 0.5$ s to show the comparison more clearly in Fig. 11 c, where the proposed method also achieves the best estimation performance. Moreover, we realize the TSC estimation methods with higher SCR and SNR in Fig. 11 d, where the better estimation performance than lower SCR and SNR is achieved. The waveform optimization also improves the TSC estimation performance, as shown in Fig. 11 d. Therefore, the proposed waveform method can work well in the scenarios both with and without clutter.

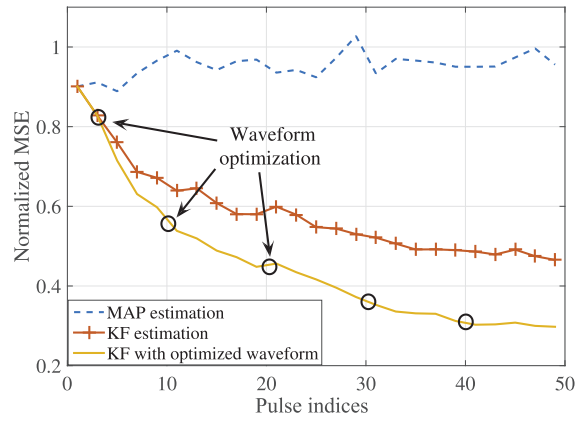
Additionally, we also illustrate the SCNR in Fig. 12. In this paper, the objective function is to minimize the MSE of estimated TSC instead of SCNR. However, by optimizing the transmitted waveform, better SCNR performance can also be achieved.

The existing methods about the waveform optimization are proposed to maximize the general parameters of received signals, such as the mutual information or SINR. Therefore, we compare the two-step optimization method with the method proposed in [9]. The method in [9] is a general method to improve the energy of echo signal from the target, and the waveform optimization method proposed in this paper is a specific method to improve the KF estimation performance. Therefore, as shown in Fig. 13, the better performance can be achieved by our method. Moreover, the proposed method is also compared with the water-filling method [10], [11], [24], and the constraints of PAPR and detection performance are not considered in the water-filling method. The proposed method in this paper optimizes the transmitted waveform directly to reduce the MSE in KF estimation, but the water-filling method is designed to improve the SCR of received signal instead of the estimation performance. Therefore, as shown in Fig. 14, the better estimation performance can be achieved using the proposed method in the scenario either with or without clutter.

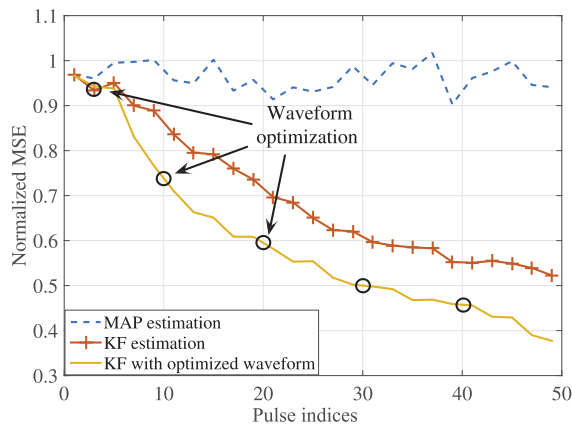
In Fig. 15, the estimation performance with the Cramér-Rao bound is given. It is shown in Fig. 15 that, as the pulse



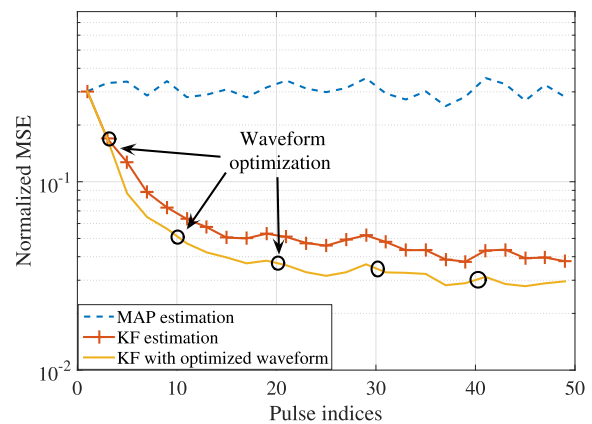
(a) Same types of target, clutter and noise ($\tau = 1$ s, SCR=-15 dB, SNR=-10 dB).



(b) Different types of target, clutter and noise ($\tau = 1$ s, SCR=-15 dB, SNR=-10 dB).



(c) Different types of target, clutter and noise ($\tau = 0.5$ s, SCR=-15 dB, SNR=-10 dB).



(d) Different types of target, clutter and noise ($\tau = 1$ s, SCR=5 dB, SNR=10 dB).

Fig. 11. TSC estimation performance with clutter.

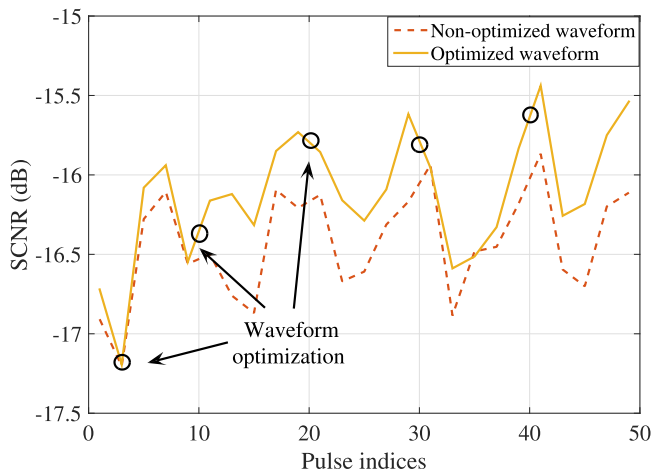


Fig. 12. The SCNR of the received signal with waveform optimization.

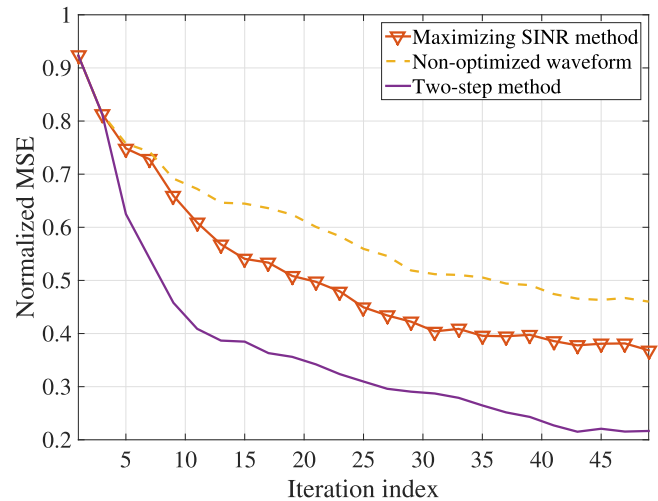


Fig. 13. The estimation performance compared with the method in [9].

number increases, the estimation performance also improves and approaches the Cramér-Rao bound. Moreover, the Cramér-Rao bound can be lower when the transmitted waveform is

optimized. Therefore, the waveform design method proposed in this paper can be efficiently used in the KF to achieve better estimation performance.

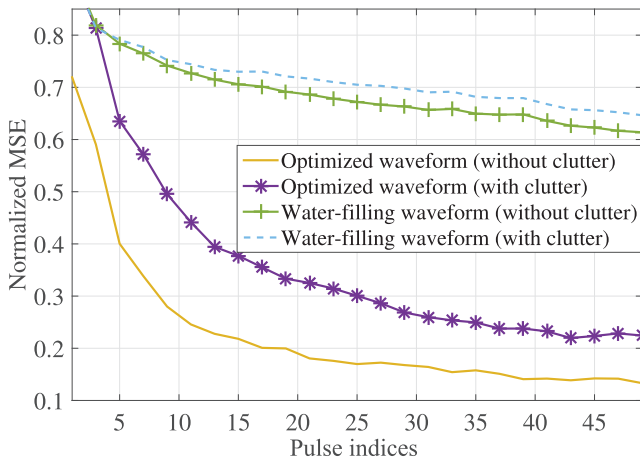


Fig. 14. The estimation performance compared with the water-filling method.

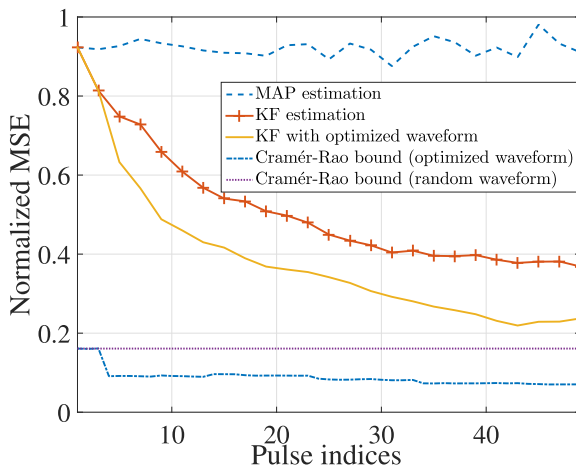


Fig. 15. The Cramér-Rao bound of the estimation methods.

VI. CONCLUSION

We have investigated the KF-based estimation method with waveform optimization in the scenario with both noise and clutter. At each KF iteration, to minimize the MSE in TSC estimation, the novel two-step method has been proposed to directly optimize the radar waveform subject to the practical constraints including the transmitted energy, the PAPR, and the target detection performance. The optimized waveform has been obtained by converting the original non-convex optimization problem into several convex problems. The simulation results demonstrate that the KF-based estimation method with optimized waveform outperforms state-of-art methods. Further work will focus on the waveform optimization for the radar systems with moving platform.

REFERENCES

- [1] S. Haykin, "Cognitive radar: A way of the future," *IEEE Signal Process. Mag.*, vol. 23, no. 1, pp. 30–40, Jan. 2006.
- [2] W. Wang, "MIMO SAR chirp modulation diversity waveform design," *IEEE Geosci. Remote Sens. Lett.*, vol. 11, no. 9, pp. 1644–1648, Apr. 2014.
- [3] P. Chen, L. Zheng, X. Wang, H. Li, and L. Wu, "Moving target detection using colocated MIMO radar on multiple distributed moving platforms," *IEEE Trans. Signal Process.*, vol. 65, no. 17, pp. 4670–4683, Jun. 2017.
- [4] A. Leshem, O. Naparstek, and A. Nehorai, "Information theoretic adaptive radar waveform design for multiple extended targets," *IEEE J. Sel. Topics Signal Process.*, vol. 1, no. 1, pp. 42–55, Jun. 2007.
- [5] F. Bandiera, M. Mancino, and G. Ricci, "Localization strategies for multiple point-like radar targets," *IEEE Trans. Signal Process.*, vol. 60, no. 12, pp. 6708–6712, Dec. 2012.
- [6] A. Aubry, A. D. Maio, D. Orlando, and M. Piezzo, "Adaptive detection of point-like targets in the presence of homogeneous clutter and subspace interference," *IEEE Signal Process. Lett.*, vol. 21, no. 7, pp. 848–852, Mar. 2014.
- [7] L. Zheng, M. Lops, and X. Wang, "Adaptive interference removal for uncoordinated radar/communication coexistence," *IEEE J. Sel. Topics Signal Process.*, vol. 12, no. 1, pp. 45–60, Feb. 2018.
- [8] M. Bell, "Information theory and radar waveform design," *IEEE Trans. Inf. Theory*, vol. 39, no. 5, pp. 1578–1597, Sep. 1993.
- [9] R. A. Romero, J. Bae, and N. A. Goodman, "Theory and application of SNR and mutual information matched illumination waveforms," *IEEE Trans. Aerosp. Electron. Syst.*, vol. 47, no. 2, pp. 912–927, Apr. 2011.
- [10] X. Zhang and C. Cui, "Range-spread target detecting for cognitive radar based on track-before-detect," *Int. J. Electron.*, vol. 101, no. 1, pp. 74–87, Jan. 2014.
- [11] F. Dai, H. Liu, P. Wang, and S. Xia, "Adaptive waveform design for range-spread target tracking," *Electron. Lett.*, vol. 46, no. 11, pp. 793–794, May 2010.
- [12] H. Jiang, J. Zhang, and K. Wong, "Joint DOD and DOA estimation for bistatic MIMO radar in unknown correlated noise," *IEEE Trans. Veh. Technol.*, vol. 64, no. 11, pp. 5113–5125, Dec. 2014.
- [13] W. Zhu and J. Tang, "Robust design of transmit waveform and receive filter for colocated MIMO radar," *IEEE Signal Process. Lett.*, vol. 22, no. 11, pp. 2112–2116, Jul. 2015.
- [14] Z. Q. Luo, W. K. Ma, A. M. C. So, Y. Y. Ye, and S. Z. Zhang, "Semidefinite relaxation of quadratic optimization problems," *IEEE Signal Process. Mag.*, vol. 27, no. 3, pp. 20–34, May 2010.
- [15] S. Sun and A. P. Petropulu, "Waveform design for MIMO radars with matrix completion," *IEEE J. Sel. Topics Signal Process.*, vol. 9, no. 8, pp. 1400–1414, Aug. 2015.
- [16] Y. Yu, S. Sun, R. N. Madan, and A. P. Petropulu, "Power allocation and waveform design for the compressive sensing based MIMO radar," *IEEE Trans. Aerosp. Electron. Syst.*, vol. 50, no. 2, pp. 898–909, Jan. 2014.
- [17] C. Chen and P. P. Vaidyanathan, "MIMO radar waveform optimization with prior information of the extended target and clutter," *IEEE Trans. Signal Process.*, vol. 57, no. 9, pp. 3533–3544, Sep. 2009.
- [18] M. Naghsh, M. Soltanalian, P. Stoica, M. Modarres-Hashemi, A. De Maio, and A. Aubry, "A doppler robust design of transmit sequence and receive filter in the presence of signal-dependent interference," *IEEE Trans. Signal Process.*, vol. 62, no. 4, pp. 772–785, Feb. 2014.
- [19] S. Imani and S. A. Ghorashi, "Transmit signal and receive filter design in co-located MIMO radar using a transmit weighting matrix," *IEEE Signal Process. Lett.*, vol. 22, no. 10, pp. 1521–1524, Mar. 2015.
- [20] S. Ahmed and M. S. Alouini, "MIMO-radar waveform covariance matrix for high SINR and low side-lobe levels," *IEEE Trans. Signal Process.*, vol. 62, no. 8, pp. 2056–2065, Feb. 2014.
- [21] P. Chen, C. Qi, L. Wu, and X. Wang, "Estimation of extended targets based on compressed sensing in cognitive radar system," *IEEE Trans. Veh. Technol.*, vol. 66, no. 2, pp. 941–951, Feb. 2017.
- [22] P. Chen, C. Qi, and L. Wu, "Antenna placement optimization for compressed sensing-based distributed MIMO radar," *IET Radar, Sonar Navigation*, vol. 11, no. 2, pp. 285–293, Apr. 2017.
- [23] F. Weinmann, "Frequency dependent RCS of a generic airborne target," in *Proc. URSI Int. Symp. Electromagn. Theory*, Berlin, Germany, Aug. 2010, pp. 977–980.
- [24] Y. Yang and R. Blum, "MIMO radar waveform design based on mutual information and minimum mean-square error estimation," *IEEE Trans. Aerosp. Electron. Syst.*, vol. 43, no. 1, pp. 330–343, Jan. 2007.
- [25] Y. Nijsure, Y. Chen, S. Boussakta, C. Yuen, Y. H. Chew, and Z. Ding, "Novel system architecture and waveform design for cognitive radar radio networks," *IEEE Trans. Veh. Technol.*, vol. 61, no. 8, pp. 3630–3642, Oct. 2012.
- [26] B. Wang, W. F. Yang, and J. K. Wang, "Adaptive waveform design for multiple radar tasks based on constant modulus constraint," *J. Appl. Math.*, vol. 2013, no. 2013, pp. 1–6, Jul. 2013.

- [27] R. Mohseni, A. Sheikhi, and M. A. Masnadi-Shirazi, "Multicarrier constant envelope OFDM signal design for radar applications," *AEU-Int. J. Electron. Commun.*, vol. 64, no. 11, pp. 999–1008, Nov. 2010.
- [28] Y. Cao and X. Xia, "IRCI-free MIMO-OFDM SAR using circularly shifted Zadoff-Chu sequences," *IEEE Geosci. Remote Sens. Lett.*, vol. 12, no. 5, pp. 1126–1130, Jan. 2015.
- [29] S. Sen, "Characterizations of PAPR-constrained radar waveforms for optimal target detection," *IEEE Sensors J.*, vol. 14, no. 5, pp. 1647–1654, May 2014.
- [30] Y. Wei, H. Meng, Y. Liu, and X. Wang, "Radar phase-coded waveform design for extended target recognition under detection constraints," in *Proc. Radar Conf.*, Kansas City, MO, USA, May 2011, pp. 1074–1079.
- [31] H. D. Meng, Y. M. Wei, X. H. Gong, Y. M. Liu, and X. Q. Wang, "Radar waveform design for extended target recognition under detection constraints," *Math. Problems Eng.*, vol. 2012, no. 2012, pp. 1–15, Nov. 2012.
- [32] M. I. Skolnik, *Radar Handbook*. New York, NY, USA: McGraw-Hill, 2009.
- [33] Q. He and R. S. Blum, "The significant gains from optimally processed multiple signals of opportunity and multiple receive stations in passive radar," *IEEE Signal Process. Lett.*, vol. 21, no. 2, pp. 180–184, Jan. 2014.
- [34] G. Y. Delisle and H. Wu, "Moving target imaging and trajectory computation using ISAR," *IEEE Trans. Aerosp. Electron. Syst.*, vol. 30, no. 3, pp. 887–899, Jul. 1994.
- [35] K. B. Petersen and M. S. Pedersen, *The Matrix Cookbook*. Lyngby, Denmark: Technical University of Denmark, Sep. 2007.
- [36] S. Boyd and L. Vandenberghe, *Convex Optimization*. Cambridge, U.K.: Cambridge Univ. Press, 2004.
- [37] S. P. Bradley, A. C. Hax, and T. L. Magnanti, *Applied Mathematical Programming*. Reading, MA, USA: Addison-Wesley, 1977.
- [38] M. Grant and S. Boyd, "CVX: MATLAB software for disciplined convex programming, version 2.1," 2014. [Online]. Available: <http://cvxr.com/cvx>
- [39] M. Grant and S. Boyd, "Graph implementations for nonsmooth convex programs," in *Recent Advances in Learning and Control*, (Series Lecture Notes in Control and Information Sciences), V. Blondel, S. Boyd, and H. Kimura, Eds. Berlin, Germany: Springer-Verlag, 2008, pp. 95–110, http://stanford.edu/boyd/graph_dcp.html
- [40] Q. He, N. H. Lehmann, R. S. Blum, and A. M. Haimovich, "MIMO radar moving target detection in homogeneous clutter," *IEEE Trans. Aerosp. Electron. Syst.*, vol. 46, no. 3, pp. 1290–1301, Jul. 2010.
- [41] U. Faigle, W. Kern, and G. Still, *Algorithmic Principles of Mathematical Programming*. Berlin, Germany: Springer-Verlag, 2013.
- [42] S. Liu, S. Chepuri, M. Fardad, E. Masazade, G. Leus, and P. Varshney, "Sensor selection for estimation with correlated measurement noise," *IEEE Trans. Signal Process.*, vol. 64, no. 13, pp. 3509–3522, Jul. 2016.
- [43] D. Zeng, *Future Intelligent Information Systems*. Berlin, Germany: Springer-Verlag, 2011.
- [44] M. Ström, M. Viberg, and K. Falk, "Wideband waveform and receiver filter bank design for clutter suppression," *IEEE J. Sel. Topics Signal Process.*, vol. 9, no. 8, pp. 1366–1376, Dec. 2015.



Peng Chen (S'15–M'17) was born in Jiangsu, China, in 1989. He received the B.E. and Ph.D. degrees both from the School of Information Science and Engineering, Southeast University, Nanjing, China, in 2011 and 2017, respectively. From March 2015 to April 2016, he was a Visiting Scholar with the Electrical Engineering Department, Columbia University, New York, NY, USA.

He is now an Associate Professor with the State Key Laboratory of Millimeter Waves, Southeast University. His research interests include radar signal processing and millimeter wave communications.



Chenhao Qi (S'06–M'10–SM'15) received the B.S. and Ph.D. degrees in signal processing from Southeast University, Nanjing, China, in 2004 and 2010, respectively.

From 2008 to 2010, he visited the Department of Electrical Engineering, Columbia University, New York, NY, USA. Since 2010, he has been with the Faculty of the School of Information Science and Engineering, Southeast University, where he is currently an Associate Professor. His research interests include sparse signal processing and wireless

communications.

Dr. Qi is an Associate Editor for the IEEE COMMUNICATIONS LETTERS and the IEEE ACCESS.



Lenan Wu received the M.S. degree in the electronics communication system from the Nanjing University of Aeronautics and Astronautics, Nanjing, China, in 1987, and the Ph.D. degree in signal and information processing from Southeast University, Nanjing, China, in 1997.

Since 1997, he has been with Southeast University, where he is a Professor, and the Director of Multimedia Technical Research Institute. He has authored or coauthored more than 400 technical papers and 11 textbooks, and is the holder of 20 Chinese patents

and 1 International patent. His research interests include multimedia information systems and communication signal processing.



Xianbin Wang (S'98–M'99–SM'06–F'17) received the Ph.D. degree in electrical and computer engineering from the National University of Singapore, Singapore, in 2001. He is currently a Professor and Tier-I Canada Research Chair with Western University, London, ON, Canada.

Prior to joining Western, he was with Communications Research Centre Canada (CRC) as a Research Scientist/Senior Research Scientist between July 2002 and December 2007. From January 2001 to July 2002, he was a System Designer with

STMicroelectronics, where he was responsible for the system design of DSL and gigabit ethernet chipsets. He has authored or coauthored more than 300 peer-reviewed journal and conference papers, in addition to 26 granted and pending patents and several standard contributions. His current research interests include 5G technologies, Internet-of-Things, communications security, machine learning, and locationing technologies. He was the recipient of many Awards and recognitions, including Canada Research Chair, CRC Presidents Excellence Award, Canadian Federal Government Public Service Award, Ontario Early Researcher Award, and five IEEE Best Paper Awards. He is currently an Editor/Associate Editor for the IEEE TRANSACTIONS ON COMMUNICATIONS, the IEEE TRANSACTIONS ON BROADCASTING, and the IEEE TRANSACTIONS ON VEHICULAR TECHNOLOGY and also an Associate Editor for the IEEE TRANSACTIONS ON WIRELESS COMMUNICATIONS between 2007 and 2011, and the IEEE WIRELESS COMMUNICATIONS LETTERS between 2011 and 2016. He was involved in many IEEE conferences including Global Communications Conference, International Conference on Communications, Vehicular Technology Conference, International Symposium on Personal, Indoor and Mobile Radio Communications, WCNC, and Canadian Workshop on Information Theory, in different roles such as symposium chair, tutorial instructor, track chair, session chair, and TPC Co-Chair. He is a fellow of Canadian Academy of Engineering and a fellow of the IEEE Distinguished Lecturer.